Proc. Natl. Acad. Sci. USA
Vol. 88, pp. 2288–2292, March 1991
Medical Sciences

Straight and paired helical filaments in Alzheimer disease have a common structural unit

(neurofibrillary tangles/neuropathology/antibody labeling/electron microscopy/image processing)

R. A. CROWTHER

Medical Research Council, Laboratory of Molecular Biology, Hills Road, Cambridge CB2 2QH, United Kingdom

Communicated by M. F. Perutz, December 20, 1990 (received for review November 12, 1990)

ABSTRACT **The presence of abundant neurofibrillary tangles in certain areas of the brain constitutes one of the defining pathological characteristics of Alzheimer disease. The predominant component of the tangle is an abnormal fibrous assembly known as the paired helical filament (PHF). The PHF is formed by a twisted double-helical ribbon of subunits that gives rise to an image alternating in width between 8 nm and 20 nm with a cross-over spacing of 80 nm. Also found in tangles is the straight filament (SF), a different kind of abnormal filament, about 15 nm wide, that does not exhibit the marked modulation in width shown by the PHF. It is reported herein that PHFs and SFs form hybrid filaments displaying both morphologies, that PHFs and SFs share surface epitopes, and that computed maps reveal a similar C-shaped morphological unit in PHFs and SFs, though differing in relative arrangement in the two types of filament. The observations imply that the SF is a structural variant of the PHF and establish a common unit of assembly for these two pathological filaments.**

Various neurological diseases are accompanied by the formation of dense fibrous aggregates within particular classes of neuron in the brain. The abnormal filaments constituting these aggregates are morphologically distinct from any of the normal components of the neuronal cytoskeleton. Little is known about the identity of the molecules that form these filaments or about the reasons for their aberrant assembly. The paired helical filament (PHF), which constitutes the principal component of neurofibrillary tangles in Alzheimer disease (1), is one of the most intensively studied of these abnormal filaments. The characteristic modulated appearance of the PHF is generated by a double-helical stack of morphological units, each with a C-shaped cross-section displaying three domains (2, 3). As seen in the electron microscope, the PHF possesses a fuzzy coat that can be stripped off by Pronase to leave a Pronase-resistant core. A monoclonal antibody (mAb 423) has been produced that decorates Pronase-stripped PHFs more strongly than unstripped PHFs (4, 5). This antibody labels a protein fragment extracted from PHF cores; sequencing and molecular cloning have identified the fragment as the repeat region of microtubule-associated protein tau (4, 6). Earlier immunological studies (7–11) showed that tau protein was associated with PHFs and some anti-tau antibodies decorate fuzzy PHFs but not stripped PHFs (5), showing that Pronase removes parts of the tau molecule lying in the fuzzy coat.

Also found in the neurofibrillary tangles of Alzheimer disease (12, 13), as a minor class, is the so-called straight filament (SF), a filament about 15 nm wide that in electron micrographs does not exhibit the marked modulation in width shown by the PHF. The term is somewhat of a misnomer as PHFs and SFs are equally straight with regard to the run of the axis, but the name SF may have been prompted by the absence of the prominently scalloped edges characteristic of images of PHFs. Antibody labeling of sectioned material and isolated filaments from Alzheimer patients has shown that SFs share epitopes with PHFs (14). The characteristic neuropathology of Alzheimer disease is also observed in middle-aged patients with Down syndrome (15), and the SFs in Down syndrome share epitopes with the PHFs of Alzheimer disease (16).

Filaments morphologically similar to Alzheimer PHFs and SFs have also been observed in Guam disease (17), in progressive supranuclear palsy (18–20), in post-encephalitic Parkinsonism (21), and in Hallervorden–Spatz disease (22). The SFs in Pick disease, a progressive senile dementia, share epitopes with the Alzheimer PHF (23), as do those of progressive supranuclear palsy (24). Thus a range of neurodegenerative diseases share common features in their filamentous pathology. However, most studies were carried out on sections of embedded tissue, in which it is difficult to observe the detailed structure of the filaments. Before concluding that the various filaments are closely related, it is necessary at the very least to analyze their fine structure in extracted preparations.

Electron micrographs shown herein of extracted SFs from patients with Alzheimer disease clearly display their morphology and indicate that hybrid filaments, part PHF and part SF, can also occur. SFs and PHFs have similar staining patterns with several antibodies and behave in a similar manner when treated with Pronase. Finally, cross-sections of SFs and PHFs computed by image processing have similarly shaped morphological units, though arranged differently in the two types of filament. Combining these observations with the fragmentation patterns of PHFs (2, 25) leads to the conclusion that PHFs and SFs represent different assemblies of an identical or closely related structural subunit.

MATERIALS AND METHODS

Filament Preparation and Electron Microscopy. Preparations for electron microscopy were made as described (4, 5). Briefly, brains were obtained post-mortem from patients with a diagnosis of Alzheimer disease, histologically confirmed by the presence of large numbers of plaques and tangles in frontal and temporal cortex. The tangle-enriched ifII fraction (4) used for microscopy was prepared by a series of differential centrifugations in nondenaturing conditions but with the inclusion of a Pronase digestion step. In some preparations used for immunostaining, the Pronase digestion step was omitted. Pronase digestion removes a fuzzy coat from the surface of the filaments, leaving behind Pronase-resistant cores that retain the characteristic morphology. Preparations were placed on carbon-coated 400-mesh grids and stained with 1% lithium phosphotungstate, and micrographs were

The publication costs of this article were defrayed in part by page charge payment. This article must therefore be hereby marked "*advertisement*" in accordance with 18 U.S.C. §1734 solely to indicate this fact.

Abbreviations: PHF, paired helical filament; SF, straight filament; mAb, monoclonal antibody.

recorded at a nominal magnification of ×45000 on a Philips model EM301 microscope.

Procedures for immunoelectron microscopy were as described (5). The primary antibodies used were the mAb NOAL 6/66.423.2 (referred to as mAb 423), raised against PHF core preparations (4), and the ICN 65-095 anti-tubulin preparation that contains substantial anti-tau activity. After reaction with the appropriate secondary antibody (Janssen Auroprobe), the grids were stained with 1% lithium phosphotungstate.

Image Processing. The micrographs were scanned by computer-linked film densitometer (26) at a spacing corresponding to about 0.45 nm on the specimen. The images of SFs were straightened and reinterpolated to give constant axial spacing between repeated features by a modification of the method described for PHFs (3). The positions of the individual repeats along the filament were located by cross-correlating a short piece corresponding to a length of 40 nm around a narrow region of the filament with the whole image. The peak heights in the cross-correlation maps alternated in strength, every second peak being higher than the intervening ones. When the short test patch was taken from the next narrow region along the image, the sets of strong and weak peaks swapped over. This indicated that the axial repeat in SFs was approximately 160 nm, corresponding to twice the 80-nm spacing between neighboring narrow regions of the filament. By using the peak positions from the cross-correlation maps, the images of the filaments were reinterpolated to straighten them and to produce repeats of constant axial length. Data corresponding to layer lines $n = 0$ to $n = 8$ of the 160-nm axial repeat and to a Fourier cutoff of 3 nm radially were extracted from the computed transforms of the three particles shown in Fig. 1 *Inset*, averaged, and used to compute three-dimensional maps with standard programs for helical particles (27, 28). Because of the low axial resolution, the computed cross-section represents an average of the structure in the axial direction and so its appearance does not change significantly through the three-dimensional map. However, the helical twist means that the projection normal to the axis does show axial variation and produces an image comparable to the original micrographs.

RESULTS

Morphological Observations. Among the PHFs in negatively stained preparations of Alzheimer neurofibrillary tangles, clearly different filaments, corresponding to SFs, were found (Fig. 1). It was hard to quantitate the overall frequency of occurrence of SFs, but it could not amount to more than a few percent of PHFs. Often SFs appeared on the electron microscope grid in small groups, either on their own or among larger groups of PHFs, suggesting that they may have assembled *in vivo* within the same cell and remained together during extraction of tangle fragments from the tissue. Comparing the images of the two kinds of filaments, the modulation in width of SFs was much less marked than that of PHFs; consequently, SFs showed a more uniform axial pattern of stain exclusion than PHFs. The average axial distance between neighboring narrow portions of the SF was about 80 nm, as it was for the PHF, though in both filaments the pitch was variable. When scanning transmission electron microscope data were being collected on unstained PHFs (5), a small number of filaments identified as SFs gave the same average mass per unit length as the PHFs, though their numbers were insufficient to obtain statistically reliable data. Fragmented SFs exhibited the same sharp transverse breaks and lack of fraying characteristic of PHFs (2).

Most importantly, searches of negatively stained preparations of tangle fragments for SFs revealed a few examples of hybrid filaments, which showed a sharp transition from a segment of PHF into a segment of SF (Fig. 2 *a* and *b*). At the transition point, one of the two strands of the PHF appeared interrupted and the SF developed on the other strand. The nicked appearance produced by the termination of one of the two strands of the PHF was seen particularly clearly in the image of the hybrid filament shown in Fig. 2*b*. The hybrid filaments are clearly different from longitudinally split PHFs (2), in which one of the two strands is missing for part of the length of the filament. The occurrence of such hybrid filaments, part PHF and part SF, implies a common structural subunit, assembled differently in PHFs and SFs.

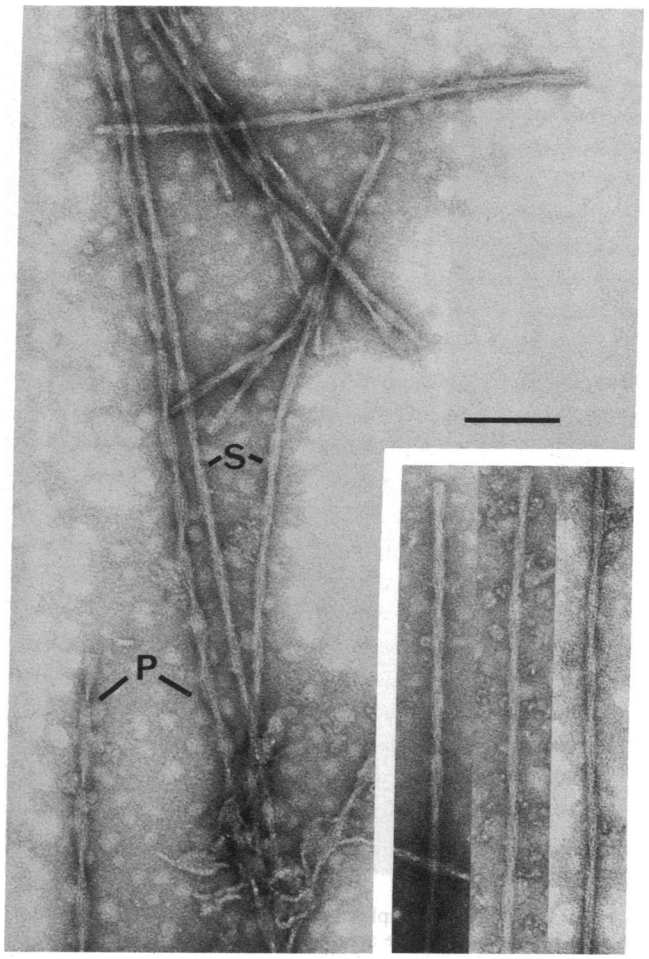

FIG. 1. Abnormal filaments in Alzheimer disease. Negatively stained PHFs (P) and SFs (S) are most clearly distinguished by viewing the electron micrograph at a glancing angle along the axis of each filament: the PHF shows narrow deeply stain-embedded regions (crossovers) alternating with much wider shallowly stain-embedded regions, whereas the SF looks more uniformly bright with much less axial modulation in the pattern of staining. (*Inset*) SFs used for computing the average cross-section shown in Fig. 3*a*. (Bar = 100 nm.)

Antibody Labeling. Labeling with antibodies supports this proposal of a common subunit. In preparations of filaments that were not treated with Pronase, both types of filament were labeled with an antiserum that contains antibodies against the microtubule-associated protein tau (Fig. 2 *c* and *d*), whereas in Pronase-treated preparations neither filament type was labeled with this antibody. On the other hand, in preparations treated with Pronase, both kinds of filament were labeled with mAb 423, which identifies a fragment of tau protein in the Pronase-resistant core of the PHF (Fig. 2*e*) (4, 5). Thus both types of filament display the same tau protein epitopes and behave in a similar manner when treated with Pronase.

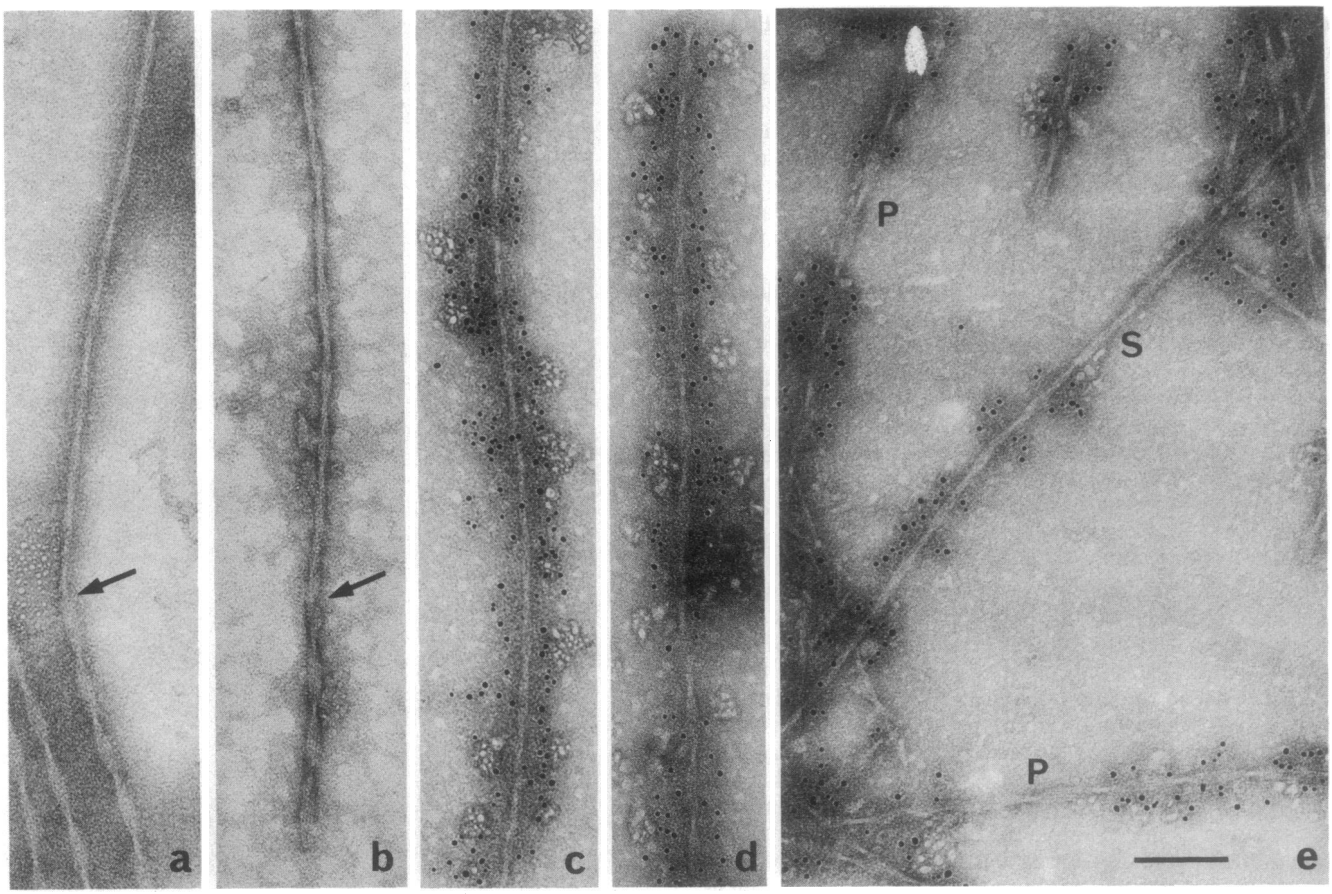

FIG. 2. (*a* and *b*) Examples of hybrid filaments. The arrows indicate the point of transition in structure from the PHF structure (below arrow) to the SF structure (above arrow). One of the two strands of the PHF appears to terminate and the SF develops on the other strand. (*c* and *d*) Filaments from an Alzheimer preparation that had not been Pronase-treated, showing decoration with an antibody with anti-tau activity (ICN anti-tubulin) visualized with electron-dense gold particles. The characteristic features of SF (*c*) and PHF (*d*) are clearly visible, despite the covering of antibodies. (*e*) Filaments from a Pronase-treated preparation lightly decorated with mAb 423 showing PHFs (P) and an SF (S) equivalently labeled. (Bar = 100 nm.)

Image Processing. By using three-dimensional image reconstruction, a cross-sectional density map of the SF was computed and compared with that computed (3) for the PHF (Fig. 3). To straighten and interpolate the filaments to constant pitch, the individual repeats were located by cross-correlating a short piece of the filament with the whole image. Although at first glance features in the images of SFs appeared to repeat in an approximate manner every 80 nm, the

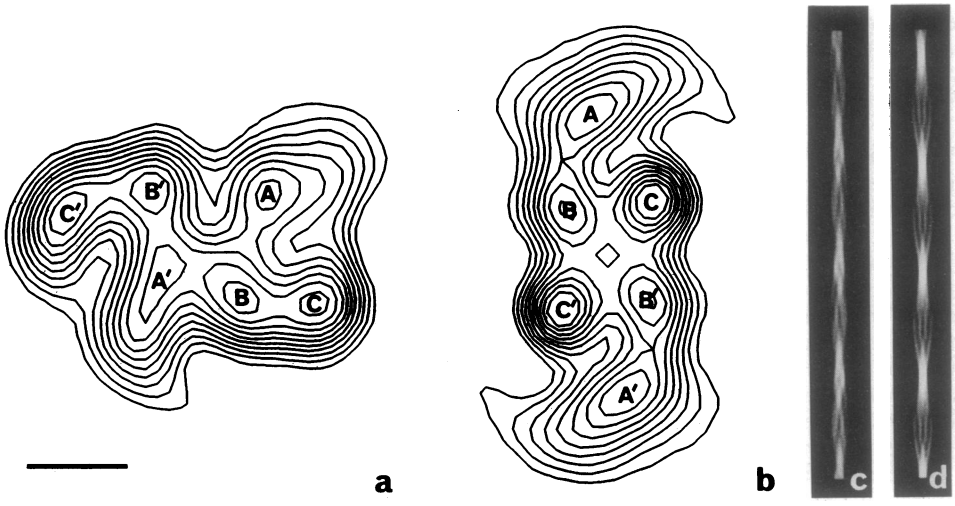

FIG. 3. Computed cross-section through the SF (*a*) compared with that found for the PHF (*b*) (3). The contour maps denote stain exclusion. Both cross-sections show two C-shaped morphological units, each displaying three peaks of density equivalently designated A, B, C and A′, B′, C′ (see text). In the SF the C-shaped units are arranged back-to-back, whereas in the PHF they are arranged base-to-base. (Bar = 4 nm.) (*c* and *d*) Projections normal to the filament axis of the image reconstructions, demonstrating how the appearances of the SF and the PHF in electron micrographs arise.

cross-correlation maps indicated that the axial repeat was actually twice this, that is, approximately 160 nm. Successive 80-nm stretches of the image were thus mirror images of one another (glide symmetry), as can be seen clearly in the computed projection shown in Fig. 3*c* and with more difficulty in the original micrographs (Fig. 1). Data corresponding to layer lines $n = 0$ to $n = 8$ of the 160-nm axial repeat were extracted from the computed transforms of the reinterpolated images of the three particles shown in Fig. 1 *Inset*, averaged, and used to compute the cross-section and projection (Fig. 3 *a* and *c*). Data were thus included to Fourier spacings of 20 nm axially and to 3 nm radially. Odd-order Bessel functions occurring on the odd-order layer lines introduced odd-order angular terms, which means that the cross-section of the SF (Fig. 3*a*) did not show a twofold axis of symmetry. By contrast, the cross-correlation maps for PHFs showed an apparent period of 80 nm, reflecting the distance between neighboring crossovers of the two strands. The low-order layer lines thus contained only even-order Bessel functions, and the computed cross-sectional map (Fig. 3*b*), therefore, showed a twofold axis of symmetry. This does not imply that the PHF would show twofold symmetry when viewed at higher resolution but simply that the images of stained filaments do not contain higher-order axial information that could break the apparent symmetry. No consistent layer-line spacings higher than $n = 8$ of the 160-nm repeat of the SF or $n = 4$ of the 80-nm repeat of the PHF were observed. The absence of higher spacings, which would give information about the axial separation of structural units in the filament, is not surprising as the stain did not appear to penetrate into the filaments in a way that defines the boundaries of the morphological unit in an axial direction. The computed maps (Fig. 3 *a* and *b*), therefore, showed details of structure in a plane normal to the axis of the filament but corresponded to an averaged structure in the axial direction.

Each cross-sectional map displayed six strong stain-excluding peaks, two of them elongated and the others almost circular. Overlaying one map on the other showed that the three peaks labeled A, B, and C (or the equivalent twofold-related set A′, B′, and C′) in the PHF could be superimposed closely on either of the two sets of three peaks labeled correspondingly in the SF (Fig. 3*a*). There were small differences of detail, not surprising at the limited resolution, but the major stain-excluding features agreed well, as did the shape of the stain-penetrated cleft between the A and C domains. The set of peaks labeled A, B, and C in the PHF constitute the C-shaped morphological unit reported by Crowther and Wischik (3). This grouping of morphological features also represents a structural unit, as longitudinal splitting along the boundary between the designated C-shaped units has been observed in PHFs themselves (2) and more clearly in untwisted forms (25); no other form of longitudinal splitting (for example, between the A and the B/C domains) has ever been observed, to my knowledge.

Thus the SF appears to be assembled from the same C-shaped structural unit as the PHF, but in the SF the C-shaped units are arranged back-to-back (interstrand contacts between A′ and B domains), whereas in the PHF they are arranged base-to-base (interstrand contacts between B and C′ domains). This means that the SF has a more nearly isometric cross-section than the PHF, so that the three-dimensional structure, viewed perpendicular to the filament, generates images in which the SF (Fig. 3*c*) shows much less variation in width than does the PHF (Fig. 3*d*), explaining their different appearances in micrographs. In both cases the computed images of filaments account well for the details of longitudinal variation of density seen in the original micrographs. A minority of images of SFs analyzed gave computed cross-sections in which the C-shaped units were laterally displaced producing B–B′ domain contacts (data not shown). The variability may reflect differences of staining or indicate the existence of a range of possible paired helical structures.

DISCUSSION

The occurrence of hybrid filaments, the possession of shared epitopes, and the presence of an identically shaped structural unit indicate that SFs and PHFs represent different, though related, assemblies of the same basic molecular entity. In fact the SF is just as much a "paired helical filament" as is the PHF itself; it is the relative disposition of the two strands of subunits that distinguishes them. The existence of hybrid filaments can now be understood, in that one of the two strands of subunits must be continuous through the transition from PHF to SF, thus maintaining the integrity of the hybrid filament, whereas the other strand is interrupted and has a PHF configuration on one side of the transition but an SF configuration on the other. Besides suggesting a common origin for both types of filament, these observations strengthen the case that the C-shaped unit, first described in PHFs by Crowther and Wischik (3), does represent a packing unit for assembly of both these abnormal filaments. At the limited resolution of this study one cannot be sure that the structural subunits forming PHFs and SFs are chemically identical, though they must be closely related but could, for example, differ in chemical modification.

The repeat regions of at least two isoforms of microtubule-associated protein tau contribute to the core structure of the PHF (4, 5, 29) but the relationship of these regions of tau protein to the stain-excluding density seen in the C-shaped morphological unit is unknown. Whether the PHF core contains other molecular species is yet to be established, though a recent report suggests that PHFs may be formed entirely from modified tau protein (30).

It is surprising that the buried surfaces in the two kinds of filament are so different. The A′–B domain contacts between the strands made in the SF are apparently very different from the B–C′ domain contacts made in the PHF; although some areas exposed on the surface of the SF are buried in the PHF and vice versa, some parts must be exposed in both to account for the common pattern of antibody labeling. The differences in packing of subunits in polymorphic forms of other helical filaments [e.g., tobacco mosaic virus (31) and glutamic dehydrogenase (32)] are much less marked. Perhaps the C-shaped unit possesses some internal symmetry or structure that makes the bonding surfaces more equivalent than they appear at first sight. Unknown factors inside the degenerating cell, possibly depending on small chemical differences or modifications, may determine whether the units form predominantly PHFs or SFs or a mixture of the two. If the relationship of SFs to PHFs established here for Alzheimer disease applies to SFs in other neurodegenerative diseases, then a common mechanism for the aberrant assembly of all these polymers is suggested, though the trigger for the process may well be disease-specific.

I thank Pat Edwards for providing ifII preparations and the micrographs in Fig. 2 *c* and *d* and Drs. Goedert, Klug, and Turnell for comments on the manuscript.

1. Kidd, M. (1963) *Nature (London)* **197**, 192–193.
2. Wischik, C. M., Crowther, R. A., Stewart, M. & Roth, M. (1985) *J. Cell Biol.* **100**, 1905–1912.
3. Crowther, R. A. & Wischik, C. M. (1985) *EMBO J.* **4**, 3661–3665.
4. Wischik, C. M., Novak, M., Thøgerson, H. C., Edwards, P. C., Runswick, M. J., Jakes, R., Walker, J. E., Milstein, C., Roth, M. & Klug, A. (1988) *Proc. Natl. Acad. Sci. USA* **85**, 4506–4510.
5. Wischik, C. M., Novak, M., Edwards, P. C., Klug, A., Tich-

elaar, W. & Crowther, R. A. (1988) *Proc. Natl. Acad. Sci. USA* **85**, 4884–4888.
6. Goedert, M., Wischik, C. M., Crowther, R. A., Walker, J. E. & Klug, A. (1988) *Proc. Natl. Acad. Sci. USA* **85**, 4051–4055.
7. Brion, J. P., Passareiro, H., Nunez, J. & Flament-Durand, J. (1985) *Arch. Biol. (1880–1985)* **95**, 229–235.
8. Delacourte, A. & Defossez, A. (1986) *J. Neurol. Sci.* **76**, 173–186.
9. Grundke-Iqbal, I., Iqbal, K., Quinlan, M., Tung, Y.-C., Zaidi, M. S. & Wisniewski, H. M. (1986) *J. Biol. Chem.* **261**, 6084–6089.
10. Kosik, K. S., Joachim, C. L. & Selkoe, D. J. (1986) *Proc. Natl. Acad. Sci. USA* **83**, 4044–4048.
11. Wood, J. G., Mirra, S. S., Pollock, N. J. & Binder, L. I. (1986) *Proc. Natl. Acad. Sci. USA* **83**, 4040–4043.
12. Yagishita, S., Itoh, Y., Nan, W. & Amano, N. (1981) *Acta Neuropathol.* **54**, 239–246.
13. Metuzals, J., Montpetit, V. & Clapin, D. F. (1981) *Cell Tissue Res.* **214**, 455–482.
14. Perry, G., Mulvihill, P., Manetto, V., Autilio-Gambetti, L. & Gambetti, P. (1987) *J. Neurosci.* **7**, 3736–3738.
15. Oliver, C. & Holland, A. J. (1986) *Psychol. Med.* **16**, 307–322.
16. Brion, J. P., Couck, A. M., Passareiro, E. & Flament-Durand, J. (1985) *J. Submicrosc. Cytol.* **17**, 89–96.
17. Hirano, A., Dembitzer, H. M., Kurland, L. T. & Zimmerman, H. M. (1968) *J. Neuropathol. Exp. Neurol.* **27**, 167–182.
18. Tomonaga, M. (1977) *Acta Neuropathol.* **37**, 177–181.
19. Yagishita, S., Itoh, Y., Amano, N., Nakano, T. & Saitoh, A. (1979) *Acta Neuropathol.* **48**, 27–30.
20. Ghatak, N. R., Nochlin, D. & Hadfield, M. G. (1980) *Acta Neuropathol.* **52**, 73–76.
21. Ishii, T. & Nakamura, Y. (1981) *Acta Neuropathol.* **55**, 59–62.
22. Eidelberg, D., Sotrel, A., Joachim, C., Selkoe, D., Forman, A., Pendlebury, W. W. & Perl, D. P. (1987) *Brain* **110**, 993–1013.
23. Perry, G., Stewart, D., Friedman, R., Manetto, V., Autilio-Gambetti, L. & Gambetti, P. (1987) *Am J. Pathol.* **127**, 559–568.
24. Bancher, C., Lassmann, H., Budka, H., Grundke-Iqbal, I., Iqbal, K., Wiche, G., Seitelberger, F. & Wisniewski, H. M. (1987) *Acta Neuropathol.* **74**, 39–46.
25. Crowther, R. A. (1991) *Biochim. Biophys. Acta* **1096**, 1–9.
26. Arndt, U. W., Barrington Leigh, J., Mallett, J. F. W. & Twinn, K. E. (1969) *J. Phys. E Ser.* 2, **2**, 385–387.
27. DeRosier, D. J. & Moore, P. B. (1970) *J. Mol. Biol.* **52**, 355–369.
28. Crowther, R. A., Padron, R. & Craig, R. (1985) *J. Mol. Biol.* **184**, 429–439.
29. Goedert, M., Spillantini, M. G., Potier, M. C., Ulrich, J. & Crowther, R. A. (1989) *EMBO J.* **8**, 393–399.
30. Lee, V. M.-Y., Balin, B. J., Otvos, L. & Trojanowski, J. Q. (1990) *J. Cell Biol.* **111**, 435a (abstr.).
31. Champness, J. N., Bloomer, A. C., Bricogne, G., Butler, P. J. G. & Klug, A. (1976) *Nature (London)* **259**, 20–24.
32. Josephs, R. & Borisy, G. (1972) *J. Mol. Biol.* **65**, 127–155.